- 1 Modulation of antibiotic sensitivity and biofilm formation in *Pseudomonas*
- 2 *aeruginosa* by interspecies diffusible signal factor analogues
- 3
- 4 Shi-qi An¹*, Julie Murtagh², Kate B. Twomey², Manoj K. Gupta³, Timothy P.
- 5 O'Sullivan^{3,4}, Rebecca Ingram¹, Miguel A. Valvano^{1*}, Ji-liang Tang^{5*}
- 6
- ¹The Wellcome-Wolfson Institute for Experimental Medicine, Queen's University of
- 8 Belfast, Belfast BT9 7BL, UK.
- 9 ²School of Microbiology, Biosciences Institute, University College Cork, Cork,
- 10 Ireland.
- ³School of Chemistry, University College Cork, Cork, Ireland.
- 12 ⁴School of Pharmacy, University College Cork, Cork, Ireland.
- 13 ⁵State Key Laboratory for Conservation and Utilization of Subtropical Agro-
- 14 bioresources, The Key Laboratory of Ministry of Education for Microbial and Plant
- 15 Genetic Engineering, and College of Life Science and Technology, Guangxi
- 16 University, Guangxi 530004, China
- 17
- 18
- 19 *Correspondence: s.an@qub.ac.uk (SA); m.valvano@qub.ac.uk (MAV);
- 20 jltang@gxu.edu.cn(JLT)
- 21
- 22
- 23 **RUNNING TITLE:** Interference with DSF-mediated interspecies signaling
- 24
- 25 **KEY WORDS:** Polybacterial infection, cell-cell signaling, chronic infection,
- 26 antibiotic resistance
- 27

1 ABSTRACT

2	The opportunistic pathogen Pseudomonas aeruginosa can participate in inter-species
3	communication through signaling by cis-2-unsaturated fatty acids of the diffusible
4	signal factor (DSF) family. Sensing these signals involves the histidine kinase
5	PA1396 and leads to altered biofilm formation and increased tolerance to various
6	antibiotics. Here, we show that the membrane-associated sensory input domain of
7	PA1396 has five trans-membrane helices, two of which are required for DSF sensing.
8	DSF binding is associated with enhanced auto-phosphorylation of PA1396
9	incorporated into liposomes. Further, we examined the ability of synthetic DSF
10	analogues to modulate or inhibit PA1396 activity. Several of these analogues block
11	the ability of DSF to trigger auto-phosphorylation and gene expression, whereas
12	others act as inverse agonists reducing biofilm formation and antibiotic tolerance,
13	both in vitro and in murine infection models. These analogues may thus represent lead
14	compounds for novel adjuvants to improve the efficacy of existing antibiotics.
15	
16	
17	
18	
19	
20	
21	
22	
23	
24	
25	
26	
27	
28	
29	
30	
31	
32	
33	

1 INTRODUCTION

2 Antibiotic resistance, coupled with limited development of new antibiotic agents, 3 poses a significant global threat to public health, underscoring the need to find 4 alternative strategies to fight infection(1, 2, 3). These strategies include targeting the 5 signaling pathways that regulate the synthesis of microbial virulence factors and 6 approaches to improve the efficacy of existing antibiotics. Bacterial cell-cell 7 communication (quorum sensing), biofilm formation and cyclic di-GMP signaling 8 were proposed as potential targets for interference by small molecules (1-4). Anti-9 virulence factors are attractive since they do not influence bacterial growth, which 10 may reduce the selective pressure for developing resistance. 11 12 This study addresses the modulation of *Pseudomonas aeruginosa* by inter-species 13 signaling. P. aeruginosa, a widespread opportunistic human pathogen, uses two N-14 acyl homoserine lactones (3-oxo-dodecanoyl- and butanoyl-HSL) as well as the 15 quinolone signal PQS (2-heptyl-3-hydroxy-4(1H)-quinolone) as quorum sensing 16 molecules that regulate the synthesis of many virulence factors⁽⁵⁻⁸⁾. There are various 17 reports of small molecule inhibition of these pathways, with consequent effects on virulence factor synthesis^(4, 9-13). In addition to intra-species signaling, *P. aeruginosa* 18 19 can participate in inter-species signaling mediated by molecules of the diffusible 20 signal factor (DSF) family, which are *cis*-2-unsaturated fatty acids. In particular, *P*. 21 aeruginosa senses cis-11-methyl-2-dodecenoic acid (DSF) and cis-2-dodecenoic acid 22 (BDSF), which are produced by other bacteria such as *Burkholderia* species and Stenotrophomonas maltophilia but not by P. aeruginosa ^(14, 15). Sensing occurs 23 24 through a histidine kinase PA1396 and leads to altered biofilm formation and 25 increased tolerance to several antibiotics including polymyxin B^(14, 16). Mutation of 26 PA1396 in the model strain PAO1 and several clinical isolates also leads to increased 27 tolerance to polymyxins B and E, suggesting DSF negatively modulates PA1396 activity^(14, 16). Detection of DSF family molecules in polybacterial infections, such as 28 29 those associated with cystic fibrosis (CF) where P. aeruginosa is present together 30 with other bacterial species, suggests interspecies signaling occurs in vivo and may 31 therefore lead to reduced efficacy of antibiotic therapy $^{(14, 16)}$. 32

Here, we examine in more detail the role of PA1396 in sensing DSF family signals
and the potential of structural analogues of these signals to modulate PA1396 action.

1 In particular, we focus on the effects of DSF analogues on the PA1396-regulated

- 2 functions of biofilm formation and antibiotic tolerance, both *in vitro* and in murine
- 3 infection models. We demonstrate that only two of the five trans-membrane helices of
- 4 the input domain of PA1396 are required for DSF sensing, and DSF binding is
- 5 associated with enhanced PA1396 auto-phosphorylation. Furthermore, we found that
- 6 certain analogues of DSF block its ability to trigger auto-phosphorylation, which
- 7 coincide with specific alterations in the expression of a subset of *P. aeruginosa* genes,
- 8 reduction in biofilm formation and antibiotic tolerance using both *in vitro* and *in vivo*
- 9 infection models. Together, our findings indicate DSF-mediated interspecies
- 10 interactions may be influenced pharmacologically to improve the treatment of chronic
- 11 P. aeruginosa infections.
- 12

13 **RESULTS**

14 Examining the sensor input domain of PA1396 for DSF recognition

15 Although DSF perception by PA1396 requires its membrane-associated sensor input 16 domain⁽¹⁴⁾, the underlying molecular mechanism is unknown. As a first step to better 17 understand DSF sensing by PA1396, topological models of the protein were generated 18 with various prediction programs. Analyses with TMHMM, MEMSAT, SOSUI, and 19 HMMTOP suggested a topological model for PA1396 comprising five 20 transmembrane helices (TMHs), and with the N- and the C-terminus located in the 21 periplasm and cytoplasm, respectively (Fig. 1a). In contrast, TOPPRED predicted a 22 relatively large cytosolic loop and a different location in the protein for some of the 23 TMHs. To experimentally assess the PA1396 topology, we constructed translational 24 fusions expressing hybrid proteins of the PA1396 input domain with either alkaline

- 25 phosphatase (PhoA) or β-galactosidase (LacZ) reporters as topological probes for
- 26 periplasmic and cytoplasmic locations, respectively. The hybrid proteins were
- designed such that at least one fusion was placed in each predicted loop facing eitherthe periplasm or the cytoplasm (Fig. 1b).
- 29

30 Plasmids carrying hybrid constructs were mobilized into E. coli and tested for PhoA

- and LacZ activity in solid growth medium containing the substrates for either PhoA
- 32 (X-Phos) or LacZ (X-Gal), which permitted the visual estimation of the enzyme
- 33 activity of PA1396-PhoA and PA1396-LacZ fusion proteins, respectively. E. coli
- 34 expressing PhoA fusions to PA1396 at amino acid residues E4, N6, G66, A70, A137,

1 Q139 and Q141 exhibited clear PhoA⁺ phenotypes (blue colonies), whereas PhoA

2 fusions to PA1396 at amino acid residues V37, E38, G107, G109 and L205 gave rise

3 to PhoA⁻ phenotypes (white colonies). Conversely, bacteria expressing LacZ fusions

4 to PA1396 at amino acid residues V37, E38, G107, G109, L205, T240, L300 and

5 L381 exhibited LacZ⁺ phenotypes (blue colonies). In contrast, LacZ fusions to

6 PA1396 at amino acid residues E4, N6, G66, A70, A137, Q139 and Q141 resulted in

7 LacZ⁻ phenotypes (white colonies). These findings, also confirmed by quantitative

8 assays (Supplementary Table 1), fit with a model of a five-TMHs protein and the

9 topology shown in Fig. 1b.

10

11 To test whether the predicted TMHs are important for DSF sensing, we constructed 12 PA1396 derivatives with progressive truncations at the N-terminus. Each truncated 13 PA1396 gene was cloned into pBBR1MCS and the constructs introduced into a 14 PA1396 deletion mutant. Bacteria expressing each of these transconjugants were 15 examined for their ability to respond to exogenous DSF by measuring *pmrAB* gene 16 expression using a *pmr-gfp* fusion, and for polymyxin B resistance (see Methods for 17 details). Removal of the first three TMHs did not affect the ability of PA1396 to 18 respond to DSF when compared to wild-type (Fig. 1c). In contrast, any further 19 truncation led to a loss of DSF responsiveness (Fig. 1c). Western blot analysis with 20 antisera against the His₆ tag showed that all of the truncated proteins were expressed 21 to the same level as the wild type (Supplementary Fig. 1). These results suggested 22 TMHs IV and V have a role in DSF sensing by PA1396.

23

24 To identify specific residues important for DSF binding and signal transduction, we 25 first focused on those conserved in PA1396 homologues from different bacterial 26 species. Conserved or semi-conserved residues in TMHs IV and V (Supplementary 27 Fig. 2) were examined for functionality by constructing alanine replacements (or 28 serine in the case of alanine residues). Residues Y116, L117, T121, L123, L128, T135, 29 P136, W138, A140, P142, M144, L148, M149, V154, I155, P156 and Y158 were 30 replaced and the resulting variants assayed for their ability to confer response to DSF. 31 Bacteria expressing many of the variants did not exhibit significant changes in DSF 32 responsiveness. We identified a number of variants exhibiting decreased sensitivity to 33 DSF, such that higher concentrations were required to activate the *pmr-gfp* reporter 34 although significant activation occurred at concentrations in excess of 50 μ M. These

5

1 variants had alanine replacements at T121, L123, L128, P142, L148, M149, V154 and

- 2 I155. Except for P142, all the variants with reduced DSF sensitivity were altered in
- 3 positions within the last two TMHs of PA1396. Variants with combinations of alanine

4 substitutions (such as T121A/L123A/L128A) had an even further reduced sensitivity

- 5 (Fig. 1d). The observed differences in the responses to DSF by the reporter strain
- 6 could not be attributed to differential protein expression since all replacements were
- 7 expressed to the same level as the parental protein (Supplementary Fig. 1). Together,
- 8 we conclude residues in TMH-IV and TMH-V of PA1396 play a critical role in the
- 9 recognition of the DSF signal.
- 10

11 Physiochemical features of DSF important for recognition by PA1396

12 The DSF family comprises *cis*-2-unsaturated fatty acids of differing chain length, 13 methyl substitution and saturation⁽¹⁵⁾. Individual bacteria can produce multiple DSF 14 family signals, although often a single chemical species predominates. Previous work 15 showed that the configurational isomer trans-11-methyl-2-dodecenoic acid was 500-16 fold less effective than DSF in activation of *pmrAB*, whereas the corresponding 17 unsaturated fatty acids have little or no activity⁽¹⁴⁾. To examine the structural features 18 of the DSF signals important for PA1396 sensing in more detail, we synthesized a 19 panel of analogs differing from the DSF 'parent' molecule in chain length, position 20 and presence of methyl branching or with a *trans* configuration of the double bond. 21 Additional molecules were created by esterification, conversion to hydroxamic acids 22 or amides, and by incorporation of stable aromatic substituents to replace the 23 carboxylic acid moieties (see Fig. 2a). This library of structural derivatives provided a 24 platform to define key structural features important for PA1396 sensing and signal 25 transduction activity.

26

27 The activity of the molecules in this panel was assayed by determining the relative 28 fluorescence of the reporter normalized by bacterial cell density (Fig. 2b). Because the 29 minimum concentration of DSF (cis-11-methyl-2-dodecenoic acid) for significant 30 induction of *pmr-gfp* expression was 0.01 μ M, the 27 DSF derivatives were examined 31 at this concentration. The results revealed that all fatty acids with a trans 32 configuration of the double bond at the 2-position render the molecule inactive (Fig. 33 2b), consistent with previous reports indicating this configuration is critical for DSF activity ⁽¹⁶⁻¹⁸⁾. However, the presence or the position of the methyl group at C-11 in 34

1 DSF was not essential for activity. Indeed, *cis*-2-tridecenoic acid (C9) and *cis*-2-

- 2 dodecenoic acid (C2, BDSF) without the methyl substitution, as well as *cis*-7-methyl-
- 3 2-dodecenoic acid (C6) and *cis*-8-methyl-2-dodecenoic acid (C5) where the methyl
- 4 group was transposed to the C-7 and C-8 positions, were equally effective in the
- 5 bioassay. In contrast, the fatty acid chain length played a major role in determining
- 6 bioactivity. *cis*-2-Unsaturated fatty acids with chain lengths of 12-14 carbons were
- 7 active whereas those with longer chains were not (Fig. 2b). The introduction of a
- 8 second double bond in the chain also led to reduced activity, while derivatives in
- 9 which the carboxylic acid was esterified, converted to a hydroxamic acid or amide
- 10 derivative or replaced with a 2-amino pyridine moiety were all inactive. For each of
- 11 these derivatives, no activity was seen in the concentration range from 0.01 to 1000
- 12 µM. Interestingly, *cis*-2-tetradecenoic acid (C11), which is a naturally occurring
- 13 analogue first detected in *Xylella fastidiosa*⁽¹⁷⁾, was most effective in activating the
- 14 bioassay (Fig. 2c). Strains carrying the T121A/L123A/L128A replacement mutants
- 15 of PA1396 showed similar reduced responsiveness to both C11 and DSF (Fig. 2c).
- 16

17 DSF analogues interfere with DSF signaling in *P. aeruginosa*

- 18 The structural analogues unable to trigger DSF-dependent responses were assessed for
- 19 inhibitory activity against DSF signaling. For these experiments, the molecules were
- 20 screened at 10 µM using *P. aeruginosa* grown with 50 µM DSF. Several compounds,
- 21 especially C12, C23 and C24 effectively repressed *pmr-gfp* expression (Fig. 3a),
- 22 possibly acting as PA1396 receptor antagonists. None of the compounds affected
- 23 planktonic bacterial growth (Supplementary Fig. 3). Dose response assays of each of
- the three compounds revealed that compound 23 ((Z)-11-methyl-N-
- 25 (methylsulfonyl)dodec-2-enamide; C23) was the most potent DSF antagonist showing
- 26 substantial inhibition at 0.1 μ M (Fig. 3b).
- 27

28 To examine if these compounds interfere directly with signal transduction through

29 PA1396, we assessed the effects of DSF and the putative antagonists on PA1396 auto-

- 30 phosphorylation. For these experiments, MycHis-tagged PA1396 was expressed,
- 31 purified under native conditions, and reconstituted in liposomes where the protein
- 32 adopts an inside-out orientation in which the cytoplasmic histidine acceptor, histidine
- 33 kinase and receiver domains are surface exposed. The incorporation of PA1396 into
- 34 liposomes was confirmed by Western blot using anti-Myc antibody, whereas the

1 inside-out orientation can be surmised from the accessibility of ATP to the kinase site, 2 which allows auto-phosphorylation without disruption of the liposomes. Basal auto-3 phosphorylation of PA1396 in the liposomes was seen in the absence of any signal 4 molecule (Fig. 3c, Supplementary Table 2). However, the addition of DSF to 5 PA1396-loaded liposomes increased the level of auto-phosphorylation dramatically, 6 an effect not seen in the presence of C23 (Fig. 3c, Supplementary Table 2). These 7 findings suggest C23 blocks the recognition of DSF by PA1396, which normally 8 mediates increased kinase activity. The observation that the T121A/L123A/L128A 9 mutant protein had a similar level of basal auto-phosphorylation as the parental 10 PA1396, which could not increase upon addition of DSF, also supports this 11 conclusion (Fig. 3c, Supplementary Table 2). Further, the latter result agrees with the 12 observation that T121A/L123A/L128A has a substantially reduced response to DSF in 13 vivo as measured by the pmr-gfp reporter bioassay (Fig. 1d). 14 15 We previously found that DSF alters the expression levels of *P. aeruginosa* genes implicated in virulence, biofilm formation and stress tolerance ⁽¹⁴⁾. In this study, we 16 17 assessed the effect of C23 on DSF-regulated functions by qRT-PCR using a subset of 18 11 DSF-regulated genes. These included genes involved in iron uptake (PA4358, 19 PA4359) and antibiotic resistance (PA4599, PA4774–PA4777). For these experiments, 20 P. aeruginosa was grown in artificial CF sputum medium with and without DSF 21 supplementation, and with both DSF and C23. Cultures were assayed at early log 22 phase (OD_{600} of 0.6). For several of the genes tested, the addition of C23 in the 23 growth medium reduced the level of expression seen with DSF alone and in some 24 cases (e.g. PA2966, PA5505) the effects on expression were reversed (Fig. 3d). These 25 experiments were repeated with the PA1396 mutant strain, demonstrating that the 26 addition of DSF or C23 had no effect on the level of gene expression (Supplementary 27 Fig. 4). Together, the results from in vitro auto-phosphorylation experiments and 28 transcriptional profiling of a subset of PA1396-regulated genes indicate C23 interferes 29 with the PA1396 ability to sense DSF. 30 31 Interference with DSF sensing decreases biofilm formation and alters virulence 32 of P. aeruginosa in vivo 33 DSF stimulates the development of Pseudomonas aeruginosa biofilms in vitro and

34 promotes persistent infection *in vivo*^(14, 16, 18). We examined if C23 interferes with

1 biofilm formation using a co-culture system in which *P. aeruginosa* biofilms were 2 allowed to form on human lung epithelial cells upon addition of 1 µM DSF⁽¹⁶⁾. C23 at 3 concentrations as low as $0.5 \,\mu M \, C23$ led to reduced biofilm formation in the presence 4 of DSF (Fig. 4a). Intriguingly, addition of C23 alone caused a reduction of biofilm 5 development (Fig. 4a). In contrast, the PA1396 mutant formed more biofilm than the 6 parental strain, but biofilm formation was not significantly altered by either DSF or 7 C23 (Supplementary Fig. 5a). Biofilm formation on a glass surface was also assayed 8 by crystal violet staining. Similar effects of DSF and C23 on biofilm biomass as in the 9 co-culture experiments were observed (Fig. 4b) including the ability of C23 alone to 10 inhibit biofilm formation. These effects were not seen in experiments using the 11 PA1396 mutant strain (Supplementary Fig. 5b).

12

13 To determine whether C23 modulates bacterial behavior during infections, C57BL/6 14 mice were inoculated intranasally with suspensions of *P. aeruginosa* supplemented 15 with C23, DSF or C23 with DSF. As a control, bacterial inocula were suspended in 16 PBS alone. At 24 h post infection, the P. aeruginosa PAO1 bacterial load was quite 17 considerable in the control animals. However, in the presence of C23, the number of 18 bacteria was considerably reduced. With DSF alone, higher numbers of bacteria were 19 seen after 24 h than in the control (Fig. 4c), in agreement with previous trends seen in 20 other *in vivo* models ⁽¹⁶⁾. With C23 in combination with DSF, the bacterial load was 21 reduced when compared to DSF alone (Fig. 4c). Thus, C23 reduced the bacterial load 22 in this mouse model in the presence or absence of DSF.

23

To verify that C23 functions by inhibiting DSF signaling *in vivo*, we used microarray
to compare the effects of adding either DSF alone or DSF with C23 on *P. aeruginosa*gene expression during mouse lung infection relative to the gene expression of *P. aeruginosa* in the mouse lung with no compound. RNA was derived from organisms

28 isolated directly from the lung homogenates of infected mice. The results showed that

29 the expression of 68 genes was significantly altered (> 1.25-fold, $P_{adj} < 1 \times 10^{-5}$) by

30 the addition of DSF (Fig. 4d; Supplementary Table 3). While many of these

31 differentially expressed genes were originally annotated as hypothetical proteins,

32 several encode factors required by *P. aeruginosa* for growth and/or host colonization

33 of the host; these genes included norB (PA0524), popD (PA1709), sphA (PA2659)

34 and *narK* (*PA3876*). Additional regulated genes encoded factors that contribute to *P*.

1 aeruginosa virulence and biofilm formation such as the mexC (PA4599), pmr operon

- 2 (*PA4774*, *PA4776*, *PA4777*) and *exoS* (*PA3841*).
- 3
- 4 Addition of DSF and C23 significantly altered expression of 51 genes (Fig. 4d).
- 5 Comparison with the effects of DSF alone showed expression changes in 21 genes
- 6 occurred in both treatments (DSF vs DSF plus C23) with all 21 of these genes altered
- 7 in the same direction. The expression level (fold change in expression) of these genes
- 8 was reduced in DSF plus C23 treatment when compared with the DSF treatment alone
- 9 (Supplementary Table 3). Further, some genes significantly regulated by DSF showed
- 10 no significant alteration in the presence of DSF and C23. Examples of this group of
- 11 genes include *popD* (*PA1709*) and *pmr* operon genes (*PA4774*, *PA4776*, *PA4777*).
- 12 Also, various genes showed a significant alteration in expression in response to DSF
- 13 plus C23, but not to DSF alone (Fig. 4d, 4e). Selected genes were examined using
- 14 qRT-PCR to confirm the alteration in expression as revealed by the microarray (Fig.
- 4e). Together, the combined results of the experiments described above show that C23
- 16 is not only able to inhibit DSF-activated responses *in vitro* and *in vivo*, but also has a
- 17 broader effect on gene expression independent of DSF-regulated responses.
- 18

19 The effect of C23 alone on gene expression was examined in a separate experiment on

- 20 bacteria grown in artificial sputum medium in the presence or absence of the
- 21 compound at 50 µM. RNA was extracted from these cultures and the level of
- 22 expression of selected genes examined by qRT-PCR. Of the genes examined, gcdH
- 23 (PA0447) and murA (PA4450) appeared to have elevated expression as a response of
- 24 C23 addition to *P. aeruginosa* PAO1, but showed little or no response to DSF
- 25 (Supplementary Fig. 6).
- 26

27 The DSF analogue C23 improves antibiotic efficacy

- 28 Perception of DSF by *P. aeruginosa* mediated by PA1396 leads to increased
- 29 expression of the *pmrAB* operon and the concomitant increased level of resistance to
- 30 the cationic antimicrobial peptides polymyxin B and E ^(14, 16). Further, DSF increases
- 31 tolerance to polymyxin B in P. aeruginosa biofilms-airway epithelial cells co-
- 32 cultures⁽¹⁶⁾. These observations prompted us to examine the influence of C23 on the
- 33 sensitivity of *P. aeruginosa* to antibiotics. As expected, addition of DSF led to *pmrAB*
- 34 up-regulation and an increased resistance to polymyxin B (Fig. 5a, b). By contrast,

1 addition of C23 plus DSF led to a marked reduction in *pmrAB* expression and reduced 2 resistance to polymyxin B. Although the *pmrAB* expression level in response to C23 3 alone was close to wild-type, C23 did appear to slightly enhance the activity of 4 polymyxin B against PAO1 (Fig. 5a). We also examined the influence of DSF and 5 C23 singly and in combination in resistance to other classes of antibiotics used in 6 treatment of *P. aeruginosa*. Addition of DSF to the cultures led to increased resistance 7 to tobramycin and nalidixic acid but had no effect on carbapenem resistance. The 8 effect of DSF on increased tobramycin and nalidixic acid resistance was reversed by 9 C23 (Supplementary Fig. 7).

10

11 To validate these results in other strains, we examined a panel of P. aeruginosa 12 clinical isolates and the data revealed that addition of DSF led to a significant increase 13 in the expression of *pmrAB* in each of these strains (Fig. 5b). However, addition of 14 C23 reversed this DSF-induced effect in all strains, whereas C23 alone gave only 15 modest or no increase in expression. In all of these cases, changes in *pmrAB* 16 expression were associated with a concomitant alteration in resistance to polymyxin 17 B, as seen with PAO1 (Supplementary Fig. 7). Further, addition of C23 also reversed 18 DSF-induced tobramycin tolerance in the clinical isolates, which decreased in all 19 strains (Supplementary Fig. 8). The PA1396 mutant in PAO1 showed increased 20 resistance to polymyxin B, an effect that could not be reversed by addition of C23, as 21 expected. To determine whether PA1396 was also required for the response of clinical 22 isolates of *P. aeruginosa* to C23, we created *PA1396* gene disruption mutants in five 23 of them, which were selected because of their intrinsically higher level of *pmrAB* 24 expression and polymyxin resistance. None of the mutant strains responded to C23, 25 confirming the C23 antagonist effect on DSF is mediated by PA1396 (Supplementary 26 Fig. 9).

27

We also assessed the effect of C23 on the efficacy of tobramycin treatment in the C57BL/6 mouse lung infection model. Mice were infected with 1×10^7 CFU of PAO1 and treated by inhaling PBS with or without C23. Tobramycin was administered at a concentration of 30 mg/kg one hour after infection, as previously reported^(19, 20). The lung bacterial load was determined 24 h post-infection. Control mice infected with *P*. *aeruginosa* and inhaled PBS exhibited considerable colonization (Fig. 5c), which was reduced by tobramycin treatment. However, adding C23 with tobramycin resulted in a 1 larger decrease of the bacterial load than that seen with tobramycin alone (Fig. 5c).

2 The kinetics of clearance of the *PA1396* mutant strain from mice not treated with

- 3 antibiotics was similar to that of mice infected with PAO1. Together, these results
- 4 demonstrate that C23 treatment leads to reduced resistance of *P. aeruginosa*
- 5 laboratory and clinical strains to distinct antibiotics both *in vitro* and *in vivo* during
- 6 infection, an effect manifested through a functional PA1396 sensor kinase.
- 7

8 **DISCUSSION**

9 This study provides a detailed characterization of the membrane topology of PA1396

10 including the identification of its input domain, which has considerable sequence

11 similarity with the input domain of RpfC, the sensor histidine kinase for DSF-

12 mediated cell-to-cell signalling in *Xanthomonas campestris* pv. *campestris* ^(15, 23).

13 However, significant differences between PA1396 and RpfC also exist. RpfC contains

14 a short N-terminal periplasmic region implicated in DSF binding⁽²⁴⁾, suggesting DSF

15 is captured in the periplasmic space. Residue E19, which is conserved in all

16 homologues with the RpfC-related input domain, is among various key residues for

17 DSF binding in RpfC^(14, 24). In *P. aeruginosa* PA1396, the corresponding residue is E8,

18 also in the N-terminal periplasmic region. However, deletion of a significant part of

19 the N-terminal region of PA1396 has no effect on DSF sensing by *P. aeruginosa*.

20 Unlike RpfC, our results indicate the DSF binding capability of PA1396 requires

21 residues in TMHs IV and V. This suggests that DSF likely interacts with residues in

these TMHs at the membrane level.

23

24 The PA1396 recognition of DSF shares features with the CqsS system of *Vibrio*

25 cholerae, which is responsible for detection of the quorum-sensing signal CAI-1 (S-3-

26 hydroxytridecanone). Both CqsS and PA1396 have complex membrane spanning

27 domains with multiple TMHs and periplasmic and cytoplasmic loops of limited size

and both recognise ligands with alkyl chains of medium length and an amphipathic

- 29 nature. Nevertheless, substantial differences between the systems occur. In CqsS,
- 30 conserved residues in the first three (of six) TMHs are obligatory for CAI-1 ligand
- 31 binding and subsequent signal transduction. Further, residues in the fourth
- 32 transmembrane helix enable CqsS to discriminate between CAI-1 and amino-CAI-1
- 33 and residues in the fifth TMH has roles in restricting ligand head group size and tail
- 34 length⁽²⁵⁾. In contrast, PA1396 truncation experiments suggest that the first three

- 1 TMHs of the protein are dispensable for DSF perception. However, whether THMs I-
- 2 III of PA1396 have roles in detection of other ligands is unknown.
- 3

4 Previous work on interspecies signaling in P. aeruginosa demonstrated that the cis-2-5 unsaturated fatty acids DSF and BDSF trigger *pmr* gene expression, but weak or no 6 activity was observed with the *trans*-derivatives and related saturated fatty acids. Here 7 we confirm and extend the analysis of structural requirements for interspecies 8 signaling. All trans-unsaturated fatty derivatives, irrespective of chain length, had 9 little or no signaling activity on *pmr* gene expression. Similarly, any derivative 10 lacking a free carboxylic acid group (through esterification, conversion to a 11 hydroxamic acid or substitution with a 2-amino pyridine moiety) was inactive. The 12 signaling activity was not significantly affected by the position of the methyl group 13 (at position 11 in DSF) but was partially reduced by introducing a second double bond. 14 Notably, a derivative of DSF with a second double bond (*cis, cis-*11-methyldodeca-15 2,5-dienoic acid) occurs naturally in various Xanthomonas species, but also has a 16 reduced ability compared to DSF to trigger DSF-regulated genes⁽¹⁸⁾. Further, 17 interspecies signaling in *P. aeruginosa* depends on the chain length of the *cis*-18 unsaturated fatty acid; molecules with chain lengths longer than 14 (this work) and 19 less than 12^(15, 18, 21, 22) have no activity. In particular, PA1396 does not respond to 20 cis-2-decenoic acid, a molecule produced by *P. aeruginosa* and which is implicated in 21 biofilm dispersal (15, 23).

22

23 We demonstrate that DSF and cis-unsaturated fatty acid analogues enhance the 24 tolerance of *P. aeruginosa* to a range of antibiotics including polymyxins, tobramycin 25 and nalidixic acid; this action requires the sensor kinase PA1396. In contrast, Deng 26 and colleagues⁽²⁶⁾ reported that both DSF and its analogues promote sensitivity of 27 several Gram-positive pathogens including Bacillus cereus and Staphylococcus 28 aureus to various antibiotics including kanamycin and gentamicin. The molecular 29 mechanisms underlying these effects in *B. cereus* are unclear, but it is intriguing that 30 cis- and trans-2-unsaturated fatty acids are equally effective in inducing the response. 31 32 We reasoned that if DSF signaling activates expression of genes involved in antibiotic 33 tolerance, structural analogues of the molecule could act as antagonists. Accordingly,

34 we show that various effects of DSF on *P. aeruginosa* including induction of *pmr*

1 gene expression and persistence in the mouse model is antagonised by the C23 2 analogue. Antagonism of DSF action may have an application to control of P. 3 *aeruginosa* in multispecies infections with pathogens that produce DSF family signals. 4 An example is infection associated with cystic fibrosis (CF), where *P. aeruginosa* can 5 occur together with S. maltophilia and Burkholderia species, both of which produce 6 DSF and BDSF. The detection of DSF and BDSF signals at physiologically relevant 7 levels in the sputum of CF patients supports the contention that interspecies signaling 8 may occur in these infections, where it may affect the antibiotic sensitivity of P. 9 aeruginosa as suggested by in vitro experiments. 10 11 Intriguingly, C23 has additional modulating effects on *P. aeruginosa* that cannot be 12 attributed to its role as a DSF antagonist. For example, C23 affects gcdH and murA 13 expression, two genes that do not respond to DSF. C23 also affects biofilm formation, 14 both in co-culture with lung epithelial cells and in 'complex' medium, in DSF-15 independent manner and contributes to a more rapid clearance of *P. aeruginosa* from 16 the lungs of mice. More detailed molecular knowledge of the activities of PA1396 17 may afford insight into these different actions of C23. For example, can PA1396 18 sense other environmental signals for biofilm formation (in addition to DSF) perhaps 19 through TMHs I-III? Is transduction of these signals also blocked by C23? Can C23 20 alone cause reduced auto-phosphorylation of PA1396 in vivo? Our unpublished work 21 indicate the two-component regulator PA1397 is involved in signal transduction 22 beyond PA1396 (S. An, unpublished). However, the findings are not consistent with a 23 simple model in which DSF-induced phosphorylation of PA1397 directly activates 24 *pmr* gene expression, indicating that other regulatory elements are involved. Future 25 work will be directed at identifying these components. 26 27 In conclusion, pharmacological inhibition of DSF-mediated interspecies signaling in 28 *P. aeruginosa* using a DSF analogue potential has identified a potential lead 29 compounds for molecules that could be used as antibiotic adjuvants to control 30 diseases caused by this human pathogen. 31 32 33

1 MATERIALS AND METHODS

2 Bacterial strains and culture conditions

- 3 Pseudomonas aeruginosa PAO1 was obtained from the Genetic Stock Center
- 4 (http://www.pseudomonas.med.ecu.edu/)(strain PAO0001). Other bacterial strains
- 5 and plasmids used in this study are listed in Supplementary Table 4. *P. aeruginosa*
- 6 and other strains were routinely grown at 37°C in Luria–Bertani (LB) medium while
- 7 Xanthomonas campestris strains were routinely grown at 30°C in NYGB medium,
- 8 which comprises Bacteriological Peptone (Oxoid, Basingstoke, UK), 5 g l⁻¹; yeast
- 9 extract (Difco), 3 g l^{-1} and glycerol, 20 g l^{-1} . The FABL medium consists of 97%
- 10 FAB medium [(NH₄)₂SO₄, 2 g l⁻¹; Na₂HPO₄ 2H₂O, 6 g l⁻¹; KH₂PO₄, 3 g l⁻¹; NaCl,
- 11 3 g l^{-1} ; MgCl₂, 93 mg l^{-1} ; CaCl₂, 11 mg l^{-1}) and 3% L medium (Bactotryptone,
- 12 10 g l^{-1} ; yeast extract, 5 g l^{-1} ; sodium chloride, 5 g l^{-1} ; and D-glucose 1 g l^{-1}).
- 13 Cultures were also grown in artificial sputum medium which comprises: 5 g mucin
- 14 from pig stomach mucosa (Sigma), 4 g DNA (Fluka), 5.9 mg diethylene triamine
- 15 pentaacetic acid (Sigma), 5 g NaCl, 2.2 g KCl, 5 ml egg yolk emulsion (Oxoid) and
- 16 5 g amino acids per 1 l water (pH 7.0) ^(16, 19). The antibiotics used included tobramycin,
- 17 polymyxin, kanamycin, rifampicin, gentamycin, spectinomycin, nalidixic acid,
- 18 carbapenem and tetracycline at the indicated concentrations.
- 19

20 **DNA manipulation**

- 21 Molecular biological methods such as isolation of plasmid and chromosomal DNA,
- 22 PCR, plasmid transformation, as well as restriction digestion were carried out using
- 23 standard protocols. PCR products were cleaned using the Qiaquick PCR purification
- 24 kit (Qiagen) and DNA fragments were recovered from agarose gels using Qiaquick
- 25 minielute gel purification kit (Qiagen). Oligonucleotide primers were purchased from
- 26 Sigma-Genosys. Primer sequences are provided in Supplementary Table 5.
- 27

28 Cloning the *PA1396* gene

- 29 The DNA fragments encoding the full-length PA1396 protein or truncation of interest
- 30 were synthesized by Gene Oracle (Santa Clara, USA) in pGOv4 and sub-cloned into
- 31 pET47b, pME6032 or pBAD/Myc-His before transformation into *E. coli* BL21 (DE3).
- 32 Genomic regions are described in Supplementary Table 5. BL21 (DE3) cells were
- 33 grown in LB media and induced with 0.25 mM IPTG; protein overexpression was
- 34 carried out at 37°C for 1 h. Purification was achieved by Ni²⁺ affinity chromatography

using the N-terminal His6 tag.

1

2	
3	Construction of targeted PA1396–phoA and PA1396–lacZ fusions
4	Trans membrane domain (TMD) predictions of the P. aeruginosa PA1396 protein
5	were obtained using the TOPRED ⁽²⁷⁾ , TMHMM ⁽²⁸⁾ , DAS-TMFILTER ^(29, 30) SOSUI ⁽³¹⁾
6	and HMMTOP ⁽³²⁾ programs, each with their default settings.
7	
8	Suitable fusion sites in the periplasmic and cytoplasmic loops were identified using a
9	consensus based on the TMS prediction data obtained (Supplementary Fig. 1). The
10	sites selected correspond to amino acids E4, N6, V37, E38, G66, A70, G107, G109,
11	A137, Q139, Q141 and L205. The DNA fragments encoding the proteins of interest
12	were synthesized by Gene Oracle (Santa Clara, USA) in pGOv4 and sub-cloned into
13	topology reporter plasmids <i>phoA</i> (pRMCD28) and <i>lacZ</i> (pRMCD70). Genomic
14	regions are described in Supplementary Table 5.
15	
16	The fusion junction of each construct was confirmed by sequencing. Alkaline
17	phosphatase assays were carried out according to Daniels <i>et al.</i> (1998) ⁽³³⁾ . β -Gal
18	assays were carried out according to Baker et al. (1997) ⁽³⁴⁾ , except that overnight
19	cultures were sub-cultured and grown to OD<0.6 before activity assays. Samples were
20	assayed in triplicate over at least three independent experiments.
21	
22	Truncation and mutagenesis of PA1396 gene
23	To construct strains harboring truncated PA1396 alleles, we employed plasmid
24	pME6032. We amplified <i>PA1396</i> alleles with deleted for amino acids 1–35, 1–40, 1–
25	82, 1-104, 1-114, 1-136 and 1-143 respectively. These amplified fragments were
26	ligated into pME6032 using appropriate restriction sites. Primer sequences and
27	restriction sites are provided in Supplementary Table 5. The DNA fragments encoding
28	the proteins with alterations in Y116, L117, T121, L123, L128, T135, P136, W138,
29	A140, Q142, M144, L148, M149, V154, I155 and F157 were synthesized by Gene
30	Oracle (Santa Clara, USA) in pGOv4 and sub-cloned pME6032. All constructed
31	plasmids were transformed into strain PA1396 mutant selecting for Gm ^R .
32	
33	

34

1 Synthesis of DSF analogues

2 The starting point for the synthesis of *cis*-2-dodecenoic acid C2 (BDSF) and 11-

- 3 methyldodec-2-enoic acid C1 (DSF) involved a Swern oxidation of the starting
- 4 alcohol with dimethyl sulfoxide (DMSO) and oxalyl chloride at -78 °C to
- 5 corresponding aldehydes decanal and 11-methyldecanal⁽³⁵⁾. A subsequent Wittig
- 6 reaction of the purified aldehyde with the modified Horner-Wadsworth-Emmons
- 7 phosphonate salt ethyl [bis(2,2,2-trifluoroethoxy)-phosphinyl]acetate in the presence
- 8 of sodium hydride (NaH) in THF afforded both the *cis* and *trans*- α , β -unsaturated
- 9 esters, ethyl dodec-2-enoate and ethyl 11-methyldodec-2-enoate⁽³⁶⁾. Hydrolysis of the
- 10 *cis*-α,β-unsaturated esters with lithium hydroxide (LiOH) in THF:MeOH:H₂O (2:1:1
- 11 (v/v/v)) gave required products C2 and C1^(37,38). Treatment of C1 with
- 12 propylphosphonic anhydride and cyclopropylamine gave the required amide
- 13 analogue⁽³⁹⁾. DSF antagonist C23 was prepared by way of an EDCI-mediated
- 14 coupling of C1 with methanesulfonamide in the presence of dimethylaminopyridine
- and subsequent isolation of the desired *cis*-isomer by reverse phase HPLC. All the
- 16 chemicals and reagents were purchased from Sigma-Aldrich unless otherwise stated.
- 17 Additional synthetic procedures and analytical data used in this study are delineated in
- 18 Supplementary Note.
- 19

20 **DSF** analogue structure analysis

- 21 Nuclear magnetic resonance spectra ¹H, ¹³C, ¹H-¹H COSY and DEPT were recorded
- 22 on a Bruker Avance 400 NMR Spectrometer (400 MHz for ¹H) and a Bruker Avance
- 23 500 NMR Spectrometer (500 MHz for 1H and 125 MHz for 13 C) with
- trimethylsilylchloride as an internal standard in CDCl_{3.} ¹H-¹³C correlated HMBC and
- 25 HMQC spectra were performed by Bruker Avance 500 spectrometer. Mass spectra
- 26 ESI-MS and High-Resolution Mass Spectra ESI-MS were performed on a
- 27 Waters/Micromass: LCT Premier Time of Flight and a Quattro Micro triple
- 28 quadrupole instruments respectively. Infrared spectra were measured using NaCl
- 29 plates on a Perkin Elmer paragon 1000 FT-IR spectrometer.
- 30

31 DSF bioassays

- 32 The original DSF bioassay is based on its ability to restore endoglucanase production
- 33 to *rpfF* mutant of *Xcc* as described in $^{(40)}$. DSF activity was expressed as the fold
- 34 increases in endoglucanase activity over the control. We also used the bioassay

1 previously described⁽¹⁶⁾ that relies on DSF-dependent induction of fluorescence (*pmr*-

2 gfp) in P. aeruginosa PAO1.

3

4 Reconstitution and phosphorylation of PA1396-His in liposomes

Using a variation in the method previously described^(41,42), *E. coli* strains containing
pBAD/*Myc*-His (PA1396-pBAD/*Myc*-His) were induced with 0.2% arabinose and
purified through nickel columns according to the manufacturer's instructions (Qiagen).

- 8 Liposomes were reconstituted as previously described^(24,41). Briefly, 50 mg of *E. coli*
- 9 phospholipids (44 µL of 25 mg/mL; Avanti Polar Lipids) were evaporated and then

10 dissolved into 5 ml of potassium phosphate buffer containing 80 mg of *N*-octyl- β -D-

11 glucopyranoside. The solution was dialyzed overnight against potassium phosphate

12 buffer. The resulting liposome suspension was subjected to freeze-thaw in liquid

13 nitrogen. Liposome size was analyzed by dynamic light scattering. Liposomes were

14 stored at 4 °C. Liposomes were then destabilized by the addition of 26 mg of

15 dodecylmaltoside, and 5 mg of PA1396-His (dual Myc- and His- tagged protein) was

16 added, followed by stirring at room temperature for 10 min.

17

18 Two hundred-sixty milligrams of Biobeads (BioRad) were then added to remove the 19 detergent, and the resulting solution was allowed to incubate at 4°C overnight. The 20 supernatant was then incubated with fresh Biobeads (BioRad) for 1 h in the morning. 21 The resulting liposomes containing reconstituted PA1396-His were frozen in liquid 22 N2 and stored at -80° C until used. The orientation of HKs in the liposome system 23 was established by other groups and can be confirmed from the accessibility of ATP 24 to the kinase site and anti-Myc antisera to the C-terminal PA1396-MycTag without 25 disruption of the liposomes.

26

27 Twenty microliters of the liposomes containing PA1396-His were adjusted to 10 mM 28 MgCl2 and 1 mM DTT, and various concentrations of agonist or antagonist, frozen 29 and thawed rapidly in liquid nitrogen, and kept at room temperature for 1 h (this 30 allows for the signals to be loaded within the liposomes). $[\gamma 32P]dATP (0.625 \ \mu l) (110$ 31 TBq/mmol) was added to each reaction. To some reactions, 10 μ g of PA1396-His was 32 added. At each time point (0, 10, 30, 60, or 120 min), 20 µl of SDS loading buffer was 33 added. For all experiments involving PA1396 alone, a time point of 10 min was used. 34 The samples were run on SDS/PAGE without boiling and visualized using a

- 1 Molecular Dynamics PhosphorImager. These were quantified by ImageJ software.
- 2

3 **Biofilm Assays**

- 4 Biofilm was assessed by attachment to glass and was determined by crystal violet
- staining. Log-phase-grown bacteria were diluted to OD_{600} nm = 0.02 in LB broth and
- 6 5 ml was incubated at 37°C for 24 h in 14-ml glass tubes. After gently pouring off the
- 7 media, bacterial pellicles were wash
- 8 ed twice with water and were then stained with 0.1% crystal violet. Tubes were
- 9 washed and rinsed with water until all unbound dye was removed. Bound crystal
- 10 violet was eluted in ethanol and measured at OD₅₉₅. Three independent assays were
- 11 carried out for each strain.
- 12

13 Polymyxin killing curves

- 14 Killing curves were carried out at 37°C temperature as previously described^(14, 16). In
- short, mid-log phase cultures (OD₆₀₀ 0.4–0.6) of PAO1 wild-type strain, PAO1
- 16 supplemented with 50 μ M DSF or PA1396 mutant grown in BM2 medium
- 17 supplemented with 0.5 mM and 2 mM Mg²⁺ were diluted 1:100 into 30 mM sodium
- 18 phosphate buffer, pH 7.0, containing 4 µg ml⁻¹ of polymyxin B sulphate and 5 µg ml⁻¹
- 19 polymyxin E sulphate (Sigma). Samples were shaken gently, and aliquots removed at
- 20 specified time intervals were assayed for survivors by plating appropriate dilutions
- 21 onto LB agar.
- 22

23 Infection and treatment of animals

- All animal experiments were approved by the Animal Ethics Committees of Queens
- 25 College Belfast and Nanyang Technological University. Mouse infection was
- 26 performed using a variation on the mouse model described in $^{(16, 43)}$. Briefly, *P*.
- 27 aeruginosa strains were grown in Luria broth at 37 °C overnight with shaking, after
- 28 which bacteria were collected by centrifugation and resuspended in PBS. The exact
- 29 number of bacteria was determined by plating serial dilutions of each inoculum on
- 30 pseudomonas isolation agar plates. Female C57BL/6 mice (approximately 8-weeks
- old) were anesthetized and intranasally inoculated with 20 μ l of the bacterial
- 32 suspension (1×10^7 CFU/mouse) in PBS with PAO1, PAO1/DSF, PAO1/or selected
- 33 DSF analogue or *PA1396* mutant. Mice were killed at 24 h post-infection by
- 34 intraperitoneal injection of 0.3 ml of 30% pentobarbital. Lungs were harvested

- 1 aseptically and homogenized in sterile PBS. A 10-fold serial dilution of lung
- 2 homogenates was plated on *Pseudomonas* isolation agar. The results (means±s.d.) are
- 3 expressed as CFU/lung.
- 4
- 5 For animal experiments examining the effectiveness of tobramycin treatment against
- 6 P. aeruginosa during respiratory infection, the mice were intranasally inoculated with
- 7 20 µl of the bacterial suspension in PBS with PAO1, PAO1/DSF, PAO1/or selected
- 8 DSF analogue (1×10^7 CFU/mouse). Each mouse received was administered
- 9 tobramycin 1 h post-infection. 24 h after infection, the lungs were removed,
- 10 homogenized with PBS and plated on agar to determine the number of viable bacteria.
- 11 The results (means±s.d.) are expressed as CFU/lung.
- 12

13 Gene expression-profiling experiments

- 14 For the *in vivo* RNA samples, infected animals as described above were euthanized
- 15 ~24 h post-infection. RNA was isolated from airway homogenate pellets using Trizol
- 16 according to the manufacturer's instructions. Samples were treated with DNAse, then
- 17 rRNA was removed from 1 to 5 µg of total RNA using the RiboZero kit for Gram-
- 18 negative bacteria (Epicentre). rRNA-depleted samples were concentrated by EtOH
- 19 precipitation. cDNA synthesis and hybridization to Affymetrix GeneChip P.
- 20 *aeruginosa* genome arrays were carried out by a commercial Affymetrix Genechip
- 21 service supplier (Conway Institute of Biomolecular & Biomedical Research, UCD,
- 22 Ireland). Microarray data analysis was performed using Biomedical Genomics
- 23 Workbench software (Qiagen).
- 24

25 Quantitative real-time PCR assays

- 26 P. aeruginosa strains (including mutants) were inoculated at an OD₆₀₀ of 0.1 in LB
- 27 (with 50 µM DSF-like signal molecules if used). Cultures were harvested during mid-
- log phase ($OD_{600} = 0.6$) and RNA was extracted using the High Pure RNA Isolation
- 29 Kit (Roche). The expression of genes was monitored by qRT-PCR, as described
- 30 previously ^(44,45).
- 31

32 Statistical Analysis

33 Significant differences between the means plus or minus standard deviations (SDs) of
34 different groups were examined using a two-tailed unpaired Student's *t* test. A P value

- 1 of less than 0.05 was regarded as statistically significant. All variables remained
- 2 significant after multiple testing.
- 3

4 ACKNOWLEDGMENTS

- 5 We thank Robert Ryan, Max Dow, Liang Yang and Delphine Caly for initial data,
- 6 helpful discussions and critical reading of the manuscript. Ian Gilbert and Claire
- 7 Mackenzie who provided help in resynthesizing several DSF analogues when required.
- 8 This work was supported by The Wellcome Trust grant 100204/A/12/Z.
- 9

10 AUTHOR CONTRIBUTIONS

- 11 SA designed the study. SA, JT, KBT and TPOS designed methods and experiments,
- 12 carried out the laboratory experiments, analyzed the data, interpreted the results and
- 13 wrote the paper. JT, JM, TPOS, MKG were involved in the synthesis of DSF
- 14 analogues, worked on associated data collection and their interpretation. SA and KBT
- 15 performed microarray and qPCR experiments and interpreted data. SA, KBT and RI
- 16 designed biofilm and infection experiments, discussed analyses, interpretation, and
- 17 presentation. MAV contributed to the editing and writing of the article. All authors
- 18 have contributed with edits, seen and approved the manuscript.
- 19

20 COMPETING FINANCIAL INTERESTS

- 21 The authors declare no competing financial interests.
- 22

23 ACCESSION CODES

- 24 The microarray data were deposited in the Gene Expression Omnibus (GEO) database
- 25 with series record GSE110126.
- 26
- 27
- 28
- 29
- 30
- 31
- 32
- 33
- 34

1		
2	REFE	CRENCES
3	1.	Levy SB, Marshall B (2004) Antibacterial resistance worldwide: causes,
4		challenges and responses. Nat Med 10: S122-S129.
5	2.	Taubes G (2008) The bacteria fight back. Science 321: 356-361.
6	3.	Sleator RD, Hill C (2008) Battle of the bugs. Science 321: 1294-1295.
7	4.	Sperandio V (2007) Novel approaches to bacterial a infection therapy by
8		interfering with bacteria-to-bacteria signaling. Expert Rev Anti Infect Ther 5:
9		271-276.
10	5.	Curtis MM, Russell R, Moreira CG, Adebesin AM, Wang C, Williams NS,
11		Taussig R, Stewart D, Zimmern P, Lu B, Prasad RN, Zhu C, Rasko DA,
12		Huntley JF, Falck JR, Sperandio V (2014) QseC inhibitors as an
13		antivirulence approach for Gram-negative pathogens. mBIO 5.
14	6.	Bolitho ME, Perez LJ, Koch MJ, Ng W-L, Bassler BL, Semmelhack MF.
15		(2011) Small molecule probes of the receptor binding site in the Vibrio
16		cholerae CAI-1 quorum sensing circuit. Bioorg. Med. Chem 19: 6906-6918.
17	7.	O'Loughlin CT, Miller LC, Siryaporn A, Drescher K, Semmelhack MF,
18		Bassler BL. (2013) A quorum-sensing inhibitor blocks Pseudomonas
19		aeruginosa virulence and biofilm formation. Proc Natl Acad Sci U S A.
20		110(44):17981-6.
21	8.	Williams P, Camara M (2009) Quorum sensing and environmental
22		adaptation in Pseudomonas aeruginosa: a tale of regulatory networks and
23		multifunctional signal molecules. Curr Opin Microbiol 12:182-191.
24	9.	Chugani S, Greenberg EP (2014) An evolving perspective on the
25		Pseudomonas aeruginosa orphan quorum sensing regulator QscR. Front Cell
26		Infect Microbiol 4.
27	10.	Jimenez PN, Koch G, Thompson JA, Xavier KB, Cool RH, Quax WJ
28		(2012) The multiple signaling systems regulating virulence in Pseudomonas
29		aeruginosa. Mol Biol Rev 76: 46-65.
30	11.	Bjarnsholt T, Tolker-Nielsen T, Hoiby N, Givskov M (2010) Interference of
31		Pseudomonas aeruginosa signalling and biofilm formation for infection
32		control. Expert Rev Mol Med 12.
33	12.	Jakobsen TH, van Gennip M, Phipps RK, Shanmugham MS, Christensen
34		LD, Alhede M, Skindersoe ME, Rasmussen TB, Friedrich K, Uthe F,

1		Jensen PO, Moser C, Nielsen KF, Eberl L, Larsen TO, Tanner D, Hoiby
2		N, Bjarnsholt T, Givskov M (2012) Ajoene, a sulfur-rich molecule from
3		Garlic, inhibits genes controlled by quorum sensing. Antimicrob Agents
4		Chemother 56: 2314-2325.
5	13.	Kim H-S, Lee S-H, Byun Y, Park H-D (2015) 6-Gingerol reduces
6		Pseudomonas aeruginosa biofilm formation and virulence via quorum sensing
7		inhibition. Sci Rep 5.
8	14.	Ryan RP, Fouhy Y, Garcia BF, Watt SA, Niehaus K, Yang L, Tolker-
9		Nielsen T, Dow JM (2008) Interspecies signalling via the Stenotrophomonas
10		maltophilia diffusible signal factor influences biofilm formation and
11		polymyxin tolerance in Pseudomonas aeruginosa. Mol Micro 68: 75-86.
12	15.	Ryan RP, Dow JM (2011) Communication with a growing family: diffusible
13		signal factor (DSF) signaling in bacteria. Trend Microbiol 19: 145-152.
14	16.	Twomey KB, O'Connell OJ, McCarthy Y, Dow JM, O'Toole GA, Plant
15		BJ, Ryan RP (2012) Bacterial cis-2-unsaturated fatty acids found in the cystic
16		fibrosis airway modulate virulence and persistence of Pseudomonas
17		aeruginosa. ISME J 6: 939-950.
18	17.	Beaulieu ED, Ionescu M, Chatterjee S, Yokota K, Trauner D, Lindow S
19		(2013) Characterization of a diffusible signaling factor from Xylella fastidiosa.
20		MBIO 4.
21	18.	Ryan RP, Dow JM (2008) Diffusible signals and interspecies communication
22		in bacteria. Microbiol 154: 1845-1858.
23	19.	Anderson GG, Moreau-Marquis S, Stanton BA, O'Toole GA (2008) In
24		vitro analysis of tobramycin-treated Pseudomonas aeruginosa Biofilms on
25		cystic fibrosis-derived airway epithelial cells. Infect Immun 76: 1423-1433.
26	20.	Geller DE, Pitlick WH, Nardella PA, Tracewell WG, Ramsey BW (2002)
27		Pharmacokinetics and bioavailability of aerosolized tobramycin in cystic
28		fibrosis. Chest 122: 219-226.
29	21.	Deng Y, Wu J, Eberl L, Zhang L-H (2010) Structural and functional
30		characterization of diffusible signal factor family quorum-sensing signals
31		produced by members of the Burkholderia cepacia complex. Appl Environ
32		Microbiol. 76: 4675-4683.
33	22.	Wang LH, He YW, Gao YF, Wu JE, Dong YH, He CZ, Wang SX, Weng
34		LX, Xu JL, Tay L, Fang RX, Zhang LH (2004) A bacterial cell-cell

1		communication signal with cross-kingdom structural analogues. Mol
2		Microbiol 51: 903-912.
3	23.	McCarthy Y, Yang L, Twomey KB, Sass A, Tolker-Nielsen T,
4		Mahenthiralingam E, Dow JM, Ryan RP (2010) A sensor kinase
5		recognizing the cell-cell signal BDSF (cis-2-dodecenoic acid) regulates
6		virulence in Burkholderia cenocepacia. Mol Microbiol 77: 1220-1236.
7	24.	Cai Z, Yuan ZH, Zhang H, Pan Y, Wu Y, Tian XQ, Wang FF, Wang L,
8		Qian W. (2017) Fatty acid DSF binds and allosterically activates histidine
9		kinase RpfC of phytopathogenic bacterium Xanthomonas campestris pv.
10		campestris to regulate quorum-sensing and virulence. PLoS Pathog. 2017 Apr
11		3;13(4):e1006304. doi: 10.1371/journal.ppat.1006304.
12	25.	Ng W-L, Wei Y, Perez LJ, Cong J, Long T, Koch M, Semmelhack MF,
13		Wingreen NS, Bassler BL (2010) Probing bacterial transmembrane histidine
14		kinase receptor-ligand interactions with natural and synthetic molecules. Proc
15		Natl Acad Sci USA 107:5575-5580.
16	26.	Deng Y, Lim A, Lee J, Chen S, An S, Dong Y-H, Zhang L-H (2014)
17		Diffusible signal factor (DSF) quorum sensing signal and structurally related
18		molecules enhance the antimicrobial efficacy of antibiotics against some
19		bacterial pathogens. BMC Microbiol 14.
20	27.	Vonheijne G (1992) Membrane-protein structure prediction - Hydrophobicity
21		analysis and the positive-inside rule. J Mol Biol 225: 487-494.
22	28.	Sonnhammer EL, von Heijne G, Krogh A (1998) A hidden Markov model
23		for predicting transmembrane helices in protein sequences. Intel Sys Mol Biol
24		6: 175-182.
25	29.	Cserzo M, Eisenhaber F, Eisenhaber B, Simon I (2002) On filtering false
26		positive transmembrane protein predictions. Protein Eng 15: 745-752.
27	30.	Cserzo M, Wallin E, Simon I, vonHeijne G, Elofsson A (1997) Prediction
28		of transmembrane alpha-helices in prokaryotic membrane proteins: the dense
29		alignment surface method. Protein Eng 10: 673-676.
30	31.	Hirokawa T, Boon-Chieng S, Mitaku S. (1998) SOSUI: classification and
31		secondary structure prediction system for membrane proteins. Bioinfo 14:378-
32		379.
33	32.	Tusnady GE, Simon I (2001) The HMMTOP transmembrane topology
34		prediction server. Bioinfo 17: 849-850.

1	33.	Daniels C, Vindurampulle C & Morona R (1998) Overexpression and
2		topology of the Shigella flexneri O-antigen polymerase (Rfc/Wzy). Mol
3		Microbiol 28: 1211–1222.
4	34.	Baker SJ, Daniels C & Morona R (1997) PhoP/Q regulated genes in
5		Salmonella typhi identification of melittin sensitive mutants.Microb Pathogen
6		22 : 165–179
7	35.	Tidwell TT (1990) Oxidation of alcohols by activated dimethyl-sulfoxide and
8		related reactions - an update. Synthesis 5:857-870.
9	36.	Takeda T (2004) Modern Carbonyl Olefination: Methods and Applications.
10		Wiley.
11	37.	Dayal B, Salen G, Tint GS, Shefer S, Benz SW (1990) Use of positive ion
12		fast atom bombardment mass spectrometry for rapid identification of a bile
13		alcohol glucuronide isolated from cerebrotendinous Xanthomatosis patients.
14		Steroids 55: 74-78.
15	38.	Sivasubramanian K, Kaanumalle LS, Uppili S, Ramamurthy V (2007)
16		Value of zeolites in asymmetric induction during photocyclization of
17		pyridones, cyclohexadienones and naphthalenones. Org Biomol Chem 5:
18		1569-1576.
19	39.	Montalbetti C, Falque V (2005) Amide bond formation and peptide coupling.
20		Tetrahedron 61: 10827-10852.
21	40.	Barber CE, Tang JL, Feng JX, Pan MQ, Wilson TJG, Slater H, Dow JM,
22		Williams P, Daniels MJ (1997) A novel regulatory system required for
23		pathogenicity of Xanthomonas campestris is mediated by a small diffusible
24		signal molecule. Mol Microbiol 24: 555-566.
25	41.	Clarke MB, Hughes DT, Zhu C, Boedeker EC, Sperandio V (2006) The
26		QseC sensor kinase: A bacterial adrenergic receptor. Proc Natl Acad Sci USA
27		103:10420-10425.
28	42.	Rigaud JL, Levy D (2003) Reconstitution of membrane proteins into
29		liposomes. Liposomes 372:65-86.
30	43.	McCaughey LC, Ritchie ND, Douce GR, Evans TJ, Walker D (2016)
31		Efficacy of species-specific protein antibiotics in a murine model of acute
32		Pseudomonas aeruginosa lung infection. Sci Rep. 6:30201.
33		
34		

1	44.	An S-Q, Caly DL, McCarthy Y, Murdoch SL, Ward J, Febrer M, Dow
2		JM, Ryan RP (2014) Novel cyclic di-GMP effectors of the YajQ protein
3		family control bacterial virulence. Plos Pathogens 10: e1004429.
4	45.	An S-Q, Febrer M, McCarthy Y, Tang D-J, Clissold L, Kaithakottil G,
5		Swarbreck D, Tang J-L, Rogers J, Dow JM, Ryan RP (2013) High-
6		resolution transcriptional analysis of the regulatory influence of cell-to-cell
7		signalling reveals novel genes that contribute to Xanthomonas
8		phytopathogenesis. Mol Micro 88:1058-1069.
9		
10		
11		
12		
13		
14		
15		
16		
17		
18		
19		
20		
21		
22		
23		
24		
25		
26		
27		
28		
29		
30		
31		
32		
33		
34		

1 FIGURE LEGENDS

2	Figure 1.	Membrane	topology,	trans-membrane	helices	and key	residues	of
4	rigui e i.	With moralit	topology,	ti ans-memor and	nences	anu kuy	residues	ľ

- 3 sensor kinase PA1396 involved in DSF perception.
- 4 (a) Graphical representation of the topological predictions of the position of trans-
- 5 membrane helices (TMHs) of PA1396 made by various membrane topology
- 6 prediction programs. The location of soluble segments (cytosolic or periplasmic) and
- 7 the positions of predicted TMHs are indicated. TMHs are designated by Roman
- 8 numerals.
- 9
- 10 (b) A model of membrane topology of PA1396 derived from reporter fusion data.
- 11 Phenotypes of *phoA* or *lacZa* reporter fusions together with the amino acid position at
- 12 which the reporters were fused are indicated by Green (PhoA activity) and Pink (LacZ
- 13 activity). Numbers next to each predicted TMH indicate the position of amino acid
- 14 residues at the predicted boundaries between soluble and membrane-embedded
- 15 regions.
- 16
- 17 (c) Domains of PA1396 as predicted by SMART. Domain abbreviations are: HisKA:
- 18 His Kinase A (phosphoacceptor) domain; HATPase_c: Histidine kinase-like ATPases;
- 19 REC: CheY-homologous receiver domain. Blue bars with Roman numerals indicate
- 20 different transmembrane helices. The lower part of the Figure indicates the effect of
- 21 progressive N-terminal truncation of PA1396 on the ability of the sensor to respond to
- 22 DSF, as measured by activation of *pmrAB* gene expression and resistance to
- 23 polymyxin B. DNA fragments expressing different His6-tagged constructs indicated
- 24 by the black lines were cloned into pBBR1MCS vector and introduced into the
- 25 *PA1396* mutant strain. Response to DSF and antibiotic tolerance are reported.
- 26

(d) Dose-response relationships for activation of a *pmr-gfp* transcriptional fusion by
DSF in *P. aeruginosa* strains expressing either wild-type PA1396 or representative
variants. The data shown is of a single experiment of three repeated experiments
which showed the same trend.

- 31
- 32
- 33
- 34

1	Figure 2. The biological activity of DSF analogues reveals important structural
2	features needed for perception by PA1396.
3	(a) The structure of DSF (cis-11-methyl-2-dodecenoic acid) highlighting structural
4	elements. Below this are the chemical structures of the 27 synthetic derivatives of
5	DSF, all validated by ESI-MS and ¹ H NMR spectra as described in the Methods.
6	
7	(b) The biological activity of DSF and its derivatives in activation of the <i>pmr-gfp</i>
8	fusion. Samples were tested at a concentration of 0.01 μ M (the minimum
9	concentration of cis-11-methyl-2-dodecenoic acid required for activation of the
10	bioassay). Values are the average of three repeats (mean± standard deviation).
11	
12	(c) Dose-response of DSF (cis-11-methyl-2-dodecenoic acid) and C11 (cis-2-
13	tetradecenoic acid) on activation of <i>pmr-gfp</i> transcriptional fusion in wild-type
14	PA1396 and a strain expressing the variant T121A/L123A/L128A with alteration in
15	conserved amino acids of TMH IV. The data of GFP fluorescence shown is of a
16	single experiment of three repeats which showed the same trend.
17	
18	Figure 3. DSF analogues inhibit PA1396 phosphorylation and DSF-dependent
19	activation of genes involved in virulence, antibiotic resistance and biofilm
20	formation.
21	(a) The effects of analogues (at 10 μ M) on activation of the <i>pmr-gfp</i> transcriptional
22	fusion by DSF (50 $\mu M)$ was measured as GFP fluorescence. Data shown are means of
23	three replicates and error bars indicate the standard deviations. The asterisks indicate
24	those analogues for which the level of gfp expression was significantly different from
25	that of DSF alone (** $p < 0.01$ as determined by using the Student' t test).
26	
27	(b) Dose-response relationships of the effects of selected analogues on DSF
28	activation of the pmr-gfp transcriptional fusion in wild-type Pseudomonas aeruginosa.
29	DSF was present at 50 µM. The analogues tested were C12 (cis-13-methyl
30	tetradecenoic acid), C23 (cis-11-methyl dodecenoyl methyl sulphonamide) and C24
31	(cis-11-methyl dodecenoyl cyclopropanamide). The data of GFP fluorescence shown
32	is of a single experiment of three repeats, which showed the same trend.

1	(c) PA1396 auto-phosphorylation in response to DSF and analogues. (i) Schematic
2	representation of the orientation of PA1396 in the liposome assay. Domain
3	abbreviations are: HisKA: His Kinase A (phosphoacceptor) domain; HATPase_c:
4	Histidine kinase-like ATPases; REC: CheY-homologous receiver domain. Blue bars
5	indicate different transmembrane helices. (ii) PA1396 auto-phosphorylates in the
6	liposome (lanes 1-3; which are triplicate assays), but increased phosphorylation is
7	seen in response to 10 μ M DSF (lanes 4-6); (iii) PA1396 phosphorylation in response
8	to 10 μ M DSF (lanes 1-3) is abrogated in the presence of C23 (lanes 4-6); (iv, v)
9	PA1396 (T121A/L123A/L128A) variant protein auto-phosphorylates but does not
10	response to the presence of DSF and/or C23.
11	
12	(d) Differential expression of selected genes implicated in virulence, antibiotic
13	resistance or biofilm formation in the presence DSF, C23 and DSF in combination
14	with C23. Transcript levels of PA0806, PA0901, PA1560, PA2966, PA4358, PA4359,
15	PA4599, PA4774, PA4775, PA4776 and PA5505 were examined. The qRT–PCR data
16	were normalised to 16S rRNA and are presented as the fold change with respect to the
17	wild type for each gene. Data (means \pm standard deviation) are from three
18	independent biological experiments.
19	
20	
21	
22	
23	
24	
25	
26	
27	
28	
29	
30	
31	
32	
33	

1 Figure 4. Effects of analogues on DSF-induced biofilm formation and persistence 2 of P. aeruginosa during infection. 3 (a) Effect of DSF and C23 alone or in combination on attachment of *P. aeruginosa* 4 strains to CFBE epithelial cells. For these experiments, compounds (0.5 μ M) were 5 added to the co-culture at 1h and bacterial attachment to the CFBE epithelial cells was 6 measured after 24 h (see Materials and Methods). (*P<0.01, **p<0.05, two-tailed 7 Student's *t*-test). 8 9 (b) Effect of 0.5 μ M DSF and C23 alone or in combination on attachment of *P*. 10 aeruginosa to a glass surface as assessed by crystal violet staining. Biofilm biomass is 11 measured as a ratio of absorbance at 550 and 600 nm. Values given are the mean and 12 standard deviation of triplicate measurements. Asterisks indicate values significantly 13 different from the wild-type (p<0.01, two-tailed Student's *t*-test). 14 15 (c) Effect of administration of C23 on P. aeruginosa mouse airway infection. C57BL/6 mice were infected intranasally with 1×10^7 CFU of *P. aeruginosa* PAO1 16 17 and treated by inhaling PBS with or without 50 µM C23. After 24 h infection, the 18 mice were euthanized, and bacterial loads were determined in lung homogenates. 19 Values represent the mean \pm standard deviation. Statistical significance by two tailed 20 Student's *t*-test is indicated: * *P*<0.05, ** *P*<0.01. 21 22 (d) Venn diagrams showing results of comparative transcriptome profiling of the 23 effects of addition of either DSF or DSF with C23 on gene expression in wild-type P. 24 aeruginosa during mouse lung infection. The comparator is P. aeruginosa in mouse 25 lung with no compound addition. Genes significantly up-regulated (> 1.25-fold, P_{adj} < 26 1×10^{-5}) are indicated in red, those significantly down-regulated are indicated in 27 green. The complete set of regulated genes is depicted in Supplementary Table 3. 28 29 (e) qRT-PCR analysis of expression levels of selected genes implicated in virulence 30 and biofilm formation in response to addition of DSF or DSF and C23 in wild-type P. 31 aeruginosa during mouse lung infection. Transcript levels of PA0524, PA1709, 32 PA2659, PA3876, PA4774, PA4776, PA4777 and PA3841 were examined. The gRT-33 PCR data were normalised to 16S rRNA and are presented as the fold change with

- 1 respect to the wild-type for each gene. Data (means \pm standard deviation) are
- 2 representative of three independent biological experiments.

- •

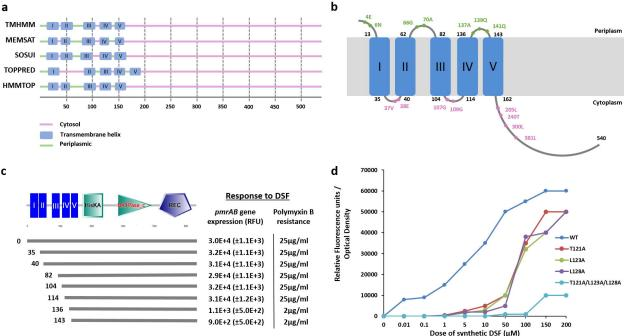
1 Figure 5. Effects of the DSF analogue C23 on antibiotic resistance of *P*.

2 *aeruginosa* both *in vitro* and during infection.

- 3 (a) Effect of addition of DSF, C23 and DSF together with C23 on tolerance of *P*.
- 4 *aeruginosa* to polymyxins. Time-courses of killing of *P. aeruginosa* by 4 μ g ml⁻¹
- 5 polymyxin B were established for bacteria suspended in sodium phosphate buffer.
- 6 Bacteria for these experiments were grown in BM2 medium with glucose
- supplemented with 2 mM Mg^{2+} . DSF and C23 were added to these cultures to a final
- 8 concentration of 50 μ M. The data shown is of a single experiment of three repeated
- 9 experiments which showed the same trend.
- 10
- 11 (b) Effect of addition of DSF, C23 and DSF with C23 on antibiotic resistance gene
- 12 expression in clinical isolates of *P. aeruginosa* as compared to the laboratory strain
- 13 PAO1. Transcript levels of PA4775 in PAO1, the isogenic PA1396 mutant and a
- selection of clinical isolates of *P. aeruginosa* (CF3, CF9, CF14, CF21 and CF 22)
- 15 were examined using qRT-PCR as described in Methods. The qRT-PCR data were
- 16 normalised to 16S rRNA and are presented as the fold change relative to the wild-type
- 17 for each gene in each strain with no addition. Data (means \pm standard deviation) are
- 18 representative of three independent biological experiments. The statistical
- 19 significance of the difference between DSF alone and C23 plus DSF or C23 alone was
- 20 examined by two tailed Student's *t*-test and are indicated as: *: *P*<0.05; **: *P*<0.01.
- 21

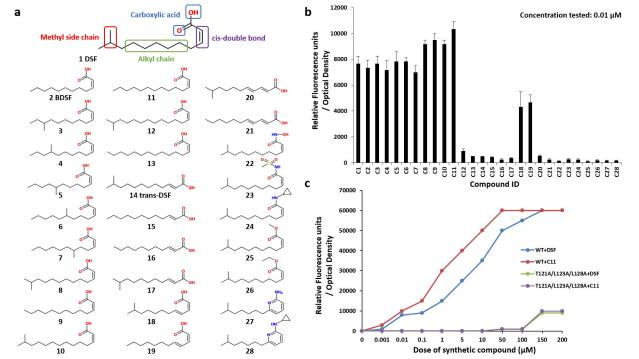
22 (c) Effect of administration of C23 on *P. aeruginosa* clearance by tobramycin

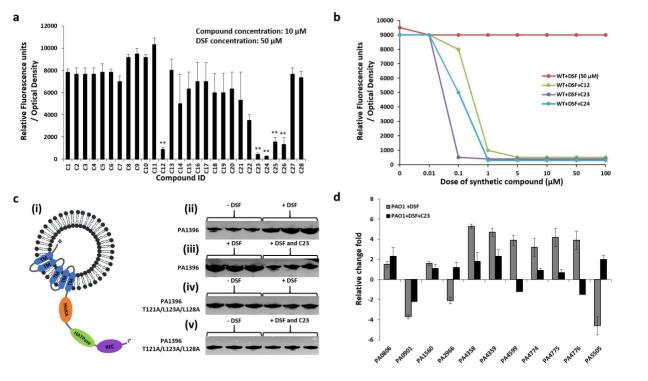
- treatment in the mouse airway. C57BL/6 mice were infected intranasally with 1×10^7
- 24 CFU *P. aeruginosa* PAO1 and treated by inhaling PBS with or without 50 µM C23.
- 25 Tobramycin was administered at a concentration of 30 mg/kg 1 h after infection. After
- 26 24 h of infection, the mice were harvested, and bacterial loads were determined in
- 27 lung homogenates. Values represent the mean \pm standard deviation. Statistical
- 28 significance of the difference between C23 plus tobramycin treatment and tobramycin
- alone was examined by two tailed Student's *t*-test and are indicated: **: *P*<0.01.

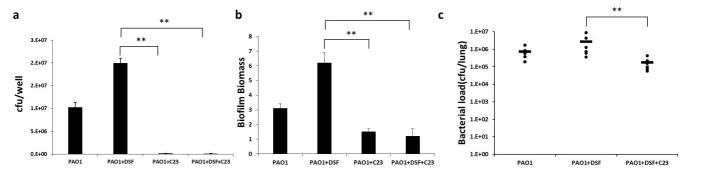


а

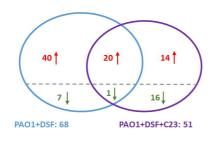
С

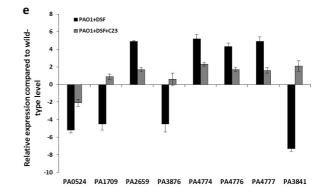


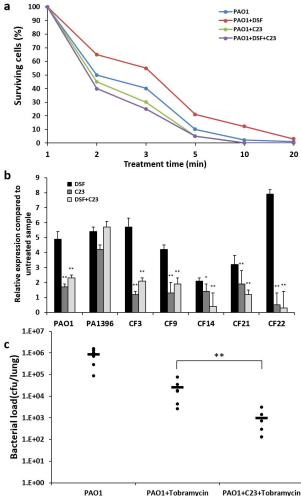












PAO1+Tobramycin PAO1+C23+Tobramycin